Pergamon

Tetrahedron: *Asymmetry* 13 (2002) 227–232

TETRAHEDRON: *ASYMMETRY*

Influence of the C(4)–C(3)–C=O dihedral angle of chiral NADH mimics on the stereoselectivity of reductions

Jean-Luc Vasse, Vincent Levacher,* Jean Bourguignon and Georges Dupas

Laboratoire de Chimie Organique, Fine et Hétérocyclique associé au CNRS, IRCOF-INSA. BP 08 F-76131, Mont Saint Aignan Cédex, France

Received 25 January 2002; accepted 22 February 2002

Abstract—Herein we report the stereoselective synthesis of new chiral NADH mimics **2** and **13** of the benzo [*b*]-1,6-naphthryridine series. The synthesis of **2** and **13** relies upon a Friedlander-type condensation between the amino imine **3** and the piperidine-2,4-dione **4** bearing a stereogenic center at C(6). The resulting NADH models were involved in the reduction of methyl benzoylformate. A comparison of their performance with that of previously reported NADH mimics such as model **1**, throws new light on the role played by the C(4)–C(3)–C=O dihedral angle (α) on the stereoselectivity of the hydride transfer.

1. Introduction

In the area of enzymatic reduction, NADH coenzyme plays an important role and has stimulated a great deal of interest in the field of biomimetic chemistry. Numerous chiral NADH models have been synthesized with a view to developing new efficient chemo- and enantioselective reducing agents and to elucidate the mechanism of the stereospecific hydrogen transfer. In the enzymatic process, it is known that depending on the nature of the enzyme, either H_R or H_S at the C(4) position of the dihydronicotinamide ring is stereospecifically transferred to a prochiral substrate. The most stable conformation of free NADH exhibits a *cis*-conformation of the carboxamide group (i.e. the C=O dipole is pointed towards the N_1 atom as depicted in Fig. 1). In contrast, X-ray structures of the coenzyme bound to enzymes show that the carboxamide group adopts a *trans* out-of-plane orientation with a dihedral angle of about 30° (α).[1] It has been suggested that the stereospecificity of the coenzyme originates from the *trans* out-of-plane orientation adopted by the carboxamide group leading to transfer of the H_{syn} hydrogen with respect to the carbonyl oxygen. An out-of-plane orientation of the amide carbonyl may be regarded as a stereogenic unit, i.e. a non-permanent chiral axis (C3–C=O) which can be partly responsible for the stereospecificity of reductions (Fig. 1).

To gain insight on how this conformational feature may contribute to the stereochemical outcome of enzymatic reductions, numerous chiral NADH mimics based on the configurational control of the C(3)–C=O chiral axis have been investigated. Among the most

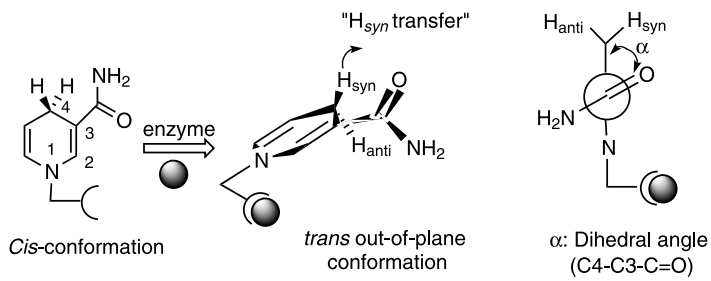

Figure 1. Conformational changes of the nicotinamide moiety in NADH coenzyme when bound to enzymes.

* Corresponding author. Fax: +33 (0) 2 35 52 29 62; e-mail: vincent.levacher@insa-rouen.fr

0957-4166/02/$ - see front matter
PII: S0957-4166(02)00101-5

representative examples of this class of models are Ohno's[2] and Vekemans'[3] reagents which were shown to be highly stereoselective in the reduction of methyl benzoylformate [(*S*) 95% e.e.]. In the course of this asymmetric reduction, a second chirality transfer occurs whereby the axial chirality of the pyridinium salt is restored with a high level of stereoselectivity [(*aS*) 95% e.e.]. This intramolecular chirality transfer is consistent with the ternary complex proposed by Vekemans in which the amide carbonyl group and the transferring hydrogen are *syn*-oriented (Fig. 2). However, the presence of an additional stereogenic unit at C(4) prevents us from assessing the role played by the C(3)–C=O chiral axis in the good performances of these NADH mimics (Fig. 2).

We recently reported[5] a new class of models in which the carbonyl amide is incorporated into a lactam structure, thereby mimicking the *trans* out-of-plane conformation adopted by the coenzyme when bound to an enzyme (Fig. 3). Molecular modeling[4] of model **1** revealed a dihedral angle of about 45°. The presence of a stereogenic center on the lactam moiety ensures the configurational control of the resulting C(3)–C=O chiral axis.[5] The stereoselective synthesis of (4*R*)-deuterated model (*aS*,*S*)-**1** gave experimental proof of D_{syn} transfer to methyl benzoylformate. Model (*aS*,*S*)-**1** afforded deuterated (*R*)-methyl mandelate with up to 84% e.e (*R*). The high level of asymmetric induction observed was ascribed to the presence of this chiral axis defined by the C(3)–C=O bond. As can be seen from the literature, numerous axially chiral NADH mimics based on the stereocontrol of the C(3)–C=O chiral axis have been reported by us and others. However, few investigations have been devoted to the influence of the C(4)–C(3)–C=O dihedral angle (α) on the enantioselective reduction of this class of NADH mimics.[6]

2. Results and discussion

In an attempt to fill in this gap, we undertook the synthesis of model **2**, which involves the carbonyl group in a six-membered lactam ring. According to molecular modeling, the most stable conformer would set both substituents R^1 and R^2 in a staggered conformation as observed in model **1**. Although both models **1** and **2** have in common many conformational and configurational features, model **2** exhibits a much smaller C(4)–C(3)–C=O dihedral angle (α) close to 10°. Models **1** and **2** offer the opportunity to study, independent of other factors, the influence of this dihedral angle on the stereoselective properties of this class of models (Fig. 3).

We intended to synthesize model **2** of the benzo[*b*]-1,6-naphthyridine series to protect the 5,6-double bond from unwanted side reactions and according to previous work in our group.[7] The target model **2** was prepared following a Friedlander quinoline synthesis.

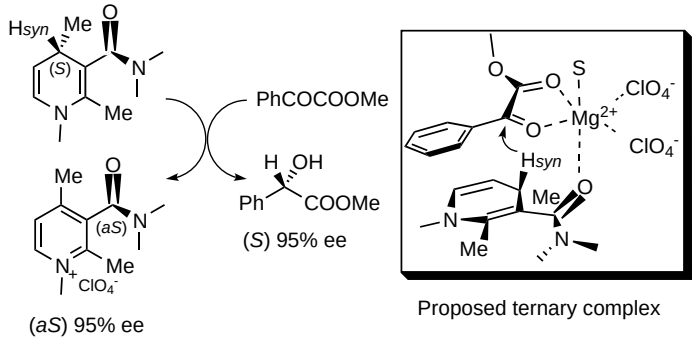

Figure 2. NADH mimics with axial and central chirality reported by Ohno[2] and Vekemans.[3]

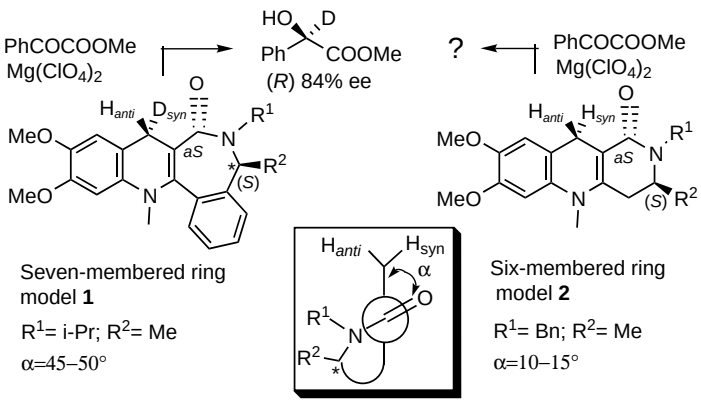

Figure 3. Design of new NADH mimics to study the relationship between the C4–C3–C=O dihedral angle (α) and the stereochemical outcome of the reduction.

The poor stability of *ortho*-aminobenzaldehydes prompted us to test the Borsche modification[8] using imine **3**.[9] The piperidine-2,4-dione **4** was obtained via Dieckmann cyclization. The rest of the synthesis follows the classical steps of quaternization and regioselective reduction of the corresponding quinolinium salt (Scheme 1).

Methods for the preparation of piperidine-2,4-diones are essentially based on Dieckmann cyclization.[10] Only few papers deal with the preparation of enantiopure piperidine-2,4-diones bearing a stereogenic center at C(6).[11] The configurational control of this stereogenic center was achieved by the known diastereoselective conjugate addition of chiral lithium amide **6** on *trans*-methyl crotonate.[12] The corresponding β-amino ester **7** was obtained in 67% yield and 95% d.e. The absolute configuration of the newly created stereogenic center was assigned as (*S*) according to literature reports.[12a] The resultant amino ester **7** was chemoselectively debenzylated to afford **8** in 95% yield. Treatment of **8** with the acid chloride derived from ethyl malonate then furnished **9** in 91% yield and Dieckmann cyclization led to the desired piperidine-2,4-dione **4**[13] in 69% yield (Scheme 2).

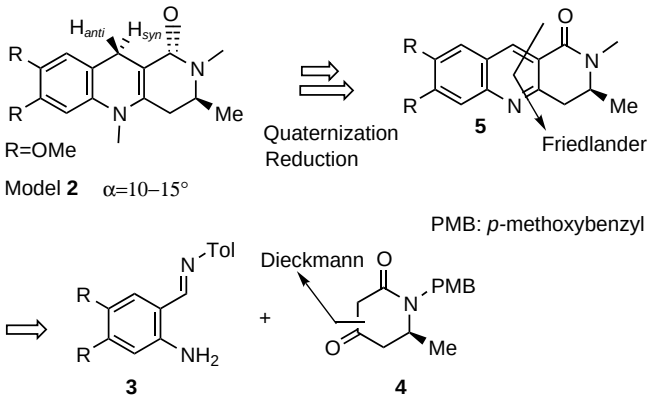

Scheme 1. Retrosynthetic analysis of model **2**.

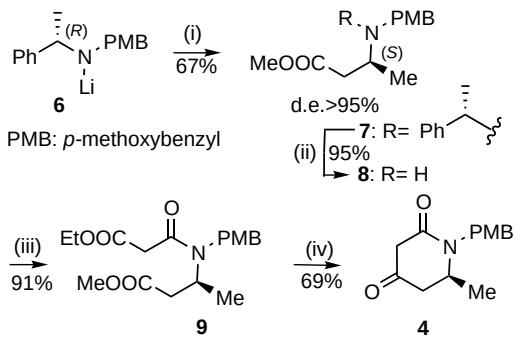

Scheme 2. *Reagents and conditions*: (i) *trans*-methyl crotonate, 30 min, –78°C; (ii) H_2, $Pd(OH)_2$, MeOH, rt, overnight; (iii) $EtOOCCH_2COCl$, NEt_3, CH_2Cl_2, rt, 6 h; (iv) MeONa, THF, Δ 2 h; then HCl (6N), Δ, 2 h.

The Friedlander reaction was achieved in refluxing ethanol in the presence of piperidine providing quinoline **5**[14] in 74% yield. The presence of the PMB group offers an additional chelation site for the magnesium ion, thereby preventing us from establishing a correlation between the dihedral angle (α) and the stereoselective properties of the models. The PMB protective group was thus cleaved under oxidative conditions to give **10** in 72% yield.[12a] Treatment of quinoline **10** with benzyl bromide furnished the benzylated quinoline **11** in 75% yield. Quaternization of the former was accomplished in nearly quantitative yield affording **12**,[15] which was subsequently reduced regioselectively under classical conditions leading to model **2**[16] (Scheme 3).

The staggered conformation of **5** placing the methyl group in a pseudo-axial position was deduced from measurement of the coupling constants between the C(3′) proton and the two C(4′) protons. Further support for this assignment came from a NOESY experiment (Fig. 4). Molecular modeling[4] confirms this finding and shows a dihedral angle (α) of about 15°. The same set of coupling constants was observed in model **2**, indicating that the methyl group occupies a pseudo-axial position as well.

Model **2** was involved in the reduction of methyl benzoylformate in the presence of magnesium perchlorate. As can be seen in Scheme 4, (*R*)-methyl mandelate was obtained with e.e. of 4%, whereas **1** led to (*R*)-methyl mandelate with up to 84% e.e. under the same condi-

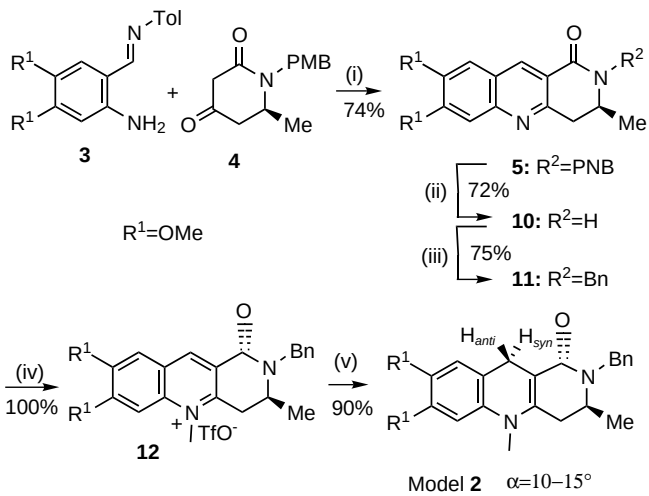

Scheme 3. *Reagents and conditions*: (i) piperidine few drops, Δ, 12 h; (ii) CAN, CH_3CN/H_2O: 9/1, rt, 4 h; (iii) KOH, benzyl bromide, DMSO, 1 h; (iv) MeOTf, CH_2Cl_2, rt; (v) $Na_2S_2O_4$, Na_2CO_3, H_2O.

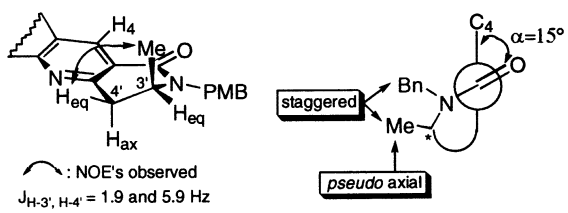

Figure 4. Conformational analysis of **5**.

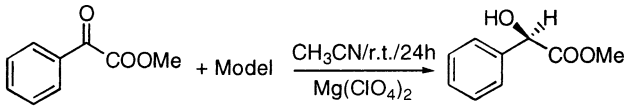

Reagent	C4-C3-C=O (α)	Yield	E.e.
Model **2**	10-15°	90%	4%(*R*)
Model **1**[a]	45-50°	95%	84%(*R*)

[a] Model **1** was previously reported in ref 5a

Scheme 4. Reduction of methyl benzoylformate.

tions (Scheme 4). Since both models **1** and **2** possess the same configurational features, this result clearly established that changes in the dihedral angle (α) lead to important variations in the stereoselectivity of reductions. One can wonder if the dihedral angle has an influence either on the stereodifferentiation of both diastereotopic C(4) protons or on the recognition of the two faces of the prochiral substrate.

Models *syn*-**13a** and *anti*-**13b** bearing a methyl group at C(4) may help to tackle this question. If both diastereotopic hydrogen atoms are effectively differentiated in model **2**, only one of the two epimers *syn*-**13a** and *anti*-**13b** should react with the substrate or at least much faster. According to the stereoselective behavior of reagent **1**,[5] one can assume that epimer *syn*-**13a**, with H-4 in a *syn* position with respect to the carbonyl group, is the most reactive (Fig. 5)

The desired tricyclic precursor **15**[17] was prepared in a similar manner with **5**, in 55% yield, by using dimethoxy aminobenzophenone **14** in a Friedländer condensation under Fehnel conditions.[18] For the same reasons as those previously mentioned with model **2**, the PMB protecting group was cleaved and the amine product **16** was subsequently benzylated to furnish **17** in 56% overall yield. Quaternization and regioselective reduction of quinolinium salt **18** by means of sodium dithionite, afforded **13a**[19] and **13b** in 91% overall yield and 80% d.e. The diastereoselectivity observed in this former step can be rationalized considering an approach of sodium dithionite to the opened face of the quinolinium salt, followed by the rearrangement of the resulting sulfinate intermediate.[20] Although the stereochemical aspect of this rearrangement has not been studied in the literature, it could be assumed that it occurs with retention of configuration. According to these considerations, the major epimer formed would be *syn*-**13a** (Scheme 5).

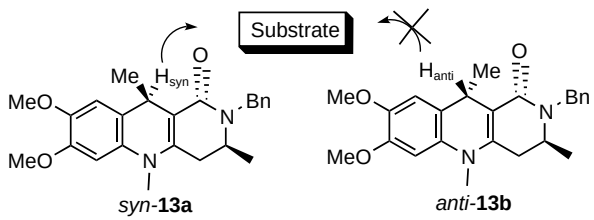

Figure 5. Difference on reactivity of both epimers **13a** and **13b** depending on the *syn* and *anti* position of H-4 with respect to the carbonyl group.

The mixture of diastereomers *syn*-**13a** and *anti*-**13b** was involved in the reduction of methyl benzoylformate under the same conditions as those applied with model **2**. The progress of the reaction was monitored, at regular intervals, by ^{1}H NMR. After two days, methyl mandelate was obtained in 80% yield with low enantioselectivity (20% e.e.) in favor of the (*R*) enantiomer (Fig. 6).

The graph in Fig. 6 clearly shows that only the major diastereomer *syn*-**13a** is consumed as methyl mandelate is formed. Since *anti*-**13b** does not participate in the reduction of the substrate, this result strongly suggests that only H_{syn} in model **2** is transferred to methyl

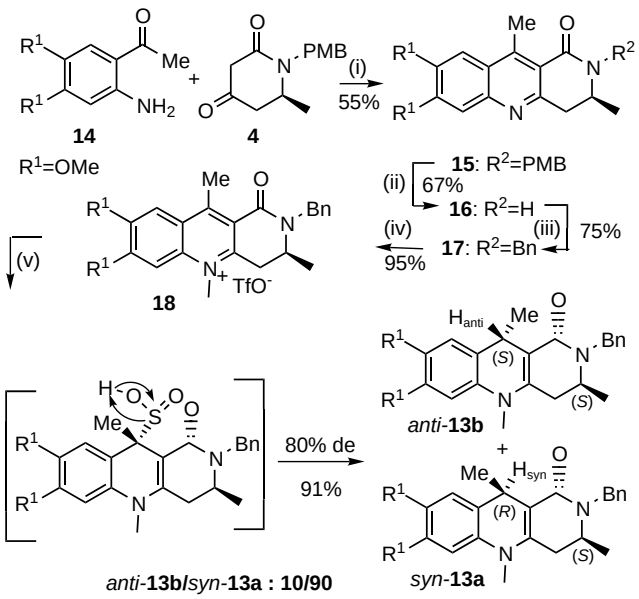

Scheme 5. Access to both epimers *syn*-**13a** and *anti*-**13b**. *Reagents and conditions*: (i) H_2SO_4 (few drops), AcOH, reflux, 2 h; (ii) CAN, CH_3CN/H_2O: 9/1, rt, 4 h; (iii) KOH, benzyl bromide, DMSO, 2 h; (iv) MeOTf, CH_2Cl_2, rt; (v) $Na_2S_2O_4$, Na_2CO_3, H_2O.

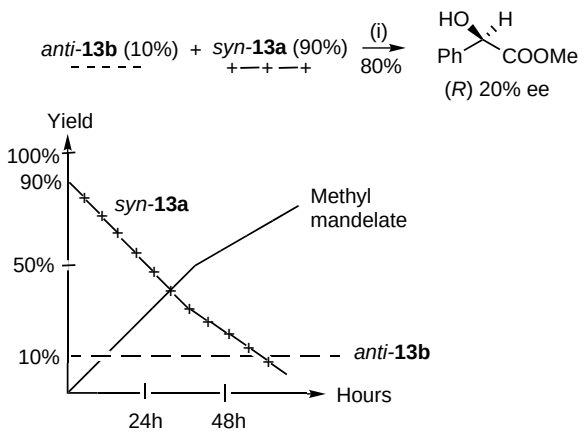

Figure 6. Reduction of methyl benzoylformate with a 90/10 mixture of epimer *syn*-**13a** and *anti*-**13b**: (i) PhCOCOOMe/$Mg(ClO_4)_2$/CH_3CN/rt/48 h.

benzoylformate, as was already demonstrated with model **1**. Consequently, decreasing the dihedral angle (α) does not affect the stereodifferentiation of both faces of the model but, has in return a dramatic effect on the stereodifferentiation of both faces of the substrate (Fig. 7a).

This study also gives further understanding on the mechanism of asymmetric induction with models previously reported by Ohno[2] and Vekemans[3] (Fig. 2, 7b). Although this class of models possess the same configurational features as those encountered in *syn*-**13a**, in particular a stereogenic center at C(4), their performances in terms of stereoselectivity are much more superior (Figs. 2 and 7b). This observation demonstrated that the stereogenic center at C(4) in Ohno's and Vekemans' models is not responsible for the stereodifferentiation of the substrate. Thus, in contrast to models **2** and *syn*-**13a**, the dihedral angle α in Ohno's and Vekemans' models close to 60° is sufficiently pronounced so that the resultant chiral relay C(3)–C=O would exert efficient stereodifferentiation of both faces of the prochiral substrate (Fig. 7b).

3. Conclusion

In summary, this work has allowed us to establish that the efficiency of axially chiral NADH mimics based on the out-of-plane orientation of the carbonyl amide is highly dependent on the dihedral angle (α). We could gain insight into the role of this resultant masked chiral axis. It confers a different reactivity of the two diastereotopic C(4) protons in favor of H_{syn} with respect to the amide carbonyl group. Moreover, the present study demonstrates that this chiral axis is effective in promoting a highly enantioselective H_{syn} transfer to methyl benzoylformate, only if it displays a fairly large dihedral angle (α). Finally, this work has important implications on the interpretation of the asymmetric induction with previously reported chiral NADH mimics bearing a carboxamide group at C(3).) In particular, these results raise the general question of the participation of this carboxamide group, as a chiral relay with this former class of models.[21]

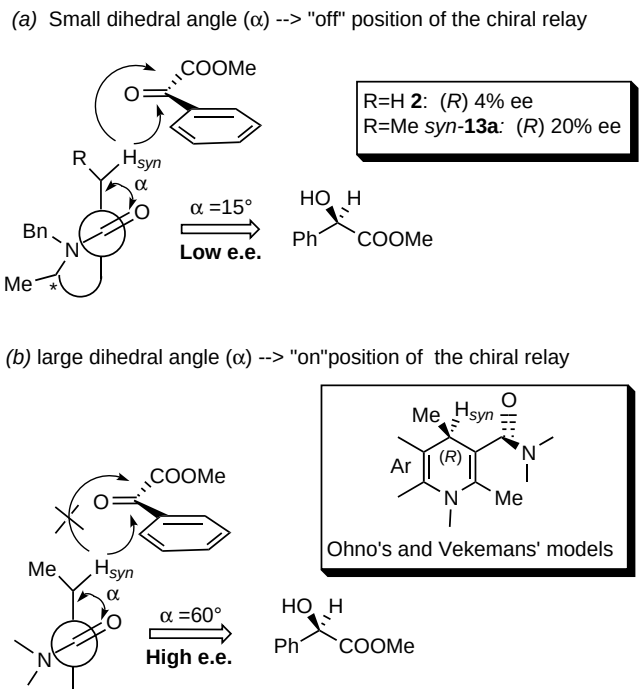

Figure 7. Relationship between the dihedral angle (α) and the stereoselective course of reduction.

Acknowledgements

We thank the CNRS, the région Haute Normandie and the CRIHAN for technical and financial support.

References

1. (a) Ecklund, H.; Samama, J. P.; Jones, T. A. *Biochemistry* **1984**, *23*, 5982; (b) Skarzynski, T.; Moody, P. C. E.; Wonacott, A. J. *J. Mol. Biol.* **1987**, *193*, 171; (c) Almarsson, Ö.; Bruice, T. C. *J. Am. Chem. Soc.* **1993**, *115*, 2125–2138; (d) Wu, Y.-D.; Houk, K. N. *J. Org. Chem.* **1993**, *58*, 2043–2045.
2. (a) Ohno, A.; Kashiwagi, M.; Ishihara, Y.; Ushida, S.; Oka, S. *Tetrahedron* **1986**, *42*, 961–973; (b) Mikita, Y.; Hayashi, K.; Mizukami, K.; Matsumoto, S.; Yano, S.; Yamazaki, N.; Ohno, A. *Tetrahedron Lett.* **2000**, *41*, 1035–1038.
3. (a) De Kok, P. M. T.; Bastiaansen, L. A. M.; van Lier, P. M.; Vekemans, J. A. J. M.; Buck, H. M. *J. Org. Chem.* **1989**, *54*, 1313–1320; (b) Buck, H. M. *Recl. Trav. Chim. Pays-Bas* **1996**, *115*, 329–332; (c) Vekemans, J. A. J. M.; Boogers, J. A. F.; Buck, H. M. *J. Org. Chem.* **1991**, *56*, 10–16.
4. PCMODEL® 7.0 implementation of MM2 force-field. CERIUS 2®, MSI CVFF force-field.
5. (a) Vasse, J. L.; Dupas, G.; Duflos, J.; Quéguiner, G.; Bourguignon, J.; Levacher, V. *Tetrahedron Lett.* **2001**, *42*, 4613–4616; (b) Vasse, J. L.; Dupas, G.; Duflos, J.; Quéguiner, G.; Bourguignon, J.; Levacher, V. *Tetrahedron Lett.* **2001**, *42*, 3713–3716.
6. (a) Bédat, J.; Levacher, V.; Dupas, G.; Quéguiner, G.; Bourguignon, J. *Chem. Lett.* **1996**, 359–360; (b) Bédat, J.; Levacher, V.; Dupas, G.; Quéguiner, G.; Bourguignon, J. *Chem. Lett.* **1995**, 327–328.
7. For previous work related to stable annelated NADH models, see: (a) Dupas, G.; Levacher, V.; Bourguignon, J.; Quéguiner, G. *Heterocycles* **1994**, *39*, 405–429; (b) Levacher, V.; Dupas, G.; Quéguiner, G.; Bourguignon, J. *Trend Heterocyclic Chem.* **1995**, *4*, 293–302; (c) Vitry, C.; Vasse, J.-L.; Dupas, G.; Levacher, V.; Quéguiner, G.; Bourguignon, J. *Tetrahedron* **2001**, *57*, 3087–3098.
8. (a) Borsche, W.; Ried, W. *Liebigs Ann. Chem.* **1943**, *554*, 269; (b) Borsche, W.; Barthenheier, J. *Liebigs Ann. Chem.* **1941**, *548*, 50.
9. Porter, H. K. The Zinin Reduction of Nitroarenes. *Org. React.* **1973**, *20*, 455–481.
10. (a) Ashton, M. J.; Hills, S. J.; Newton, C. G.; Taylor, J. B.; Tondu, S. C. D. *Heterocycles* **1989**, *28*, 1015; (b)

Micovic, I. V.; Roglic, G. M.; Ivanovic, M. D.; Dosen-Micovic, L.; Kiricojevic, V. D.; Popovic, J. B. *J. Chem. Soc., Perkin Trans. 1* **1996**, 2041.

11. (a) Waldmann, H.; Braun, M.; Dräger, M. *Tetrahedron: Asymmetry* **1991**, *2*, 1231; (b) Davies, F.; Chao, B.; Fang, T.; Szewczyk, J. M. *Org. Lett.* **2000**, *2*, 1041–1043; (c) Murray, P. J.; Starkey, I. D. *Tetrahedron Lett.* **1996**, *37*, 1875–1878; (d) Leflemme, N.; Dallemagne, P.; Rault, S. *Tetrahedron Lett.* **2001**, *42*, 8997–8999.
12. (a) Davies, S. G.; Ichihara, O. *Tetrahedron Lett.* **1998**, *39*, 6045–6048; (b) Davies, S. G.; Ichihara, O. *Tetrahedron: Asymmetry*. **1991**, *2*, 183–186.
13. Selected data for **4**: ^{1}H NMR ($CDCl_3$, 200 MHz) δ 1.19 (3H, d, $J=6.7$ Hz), 2.46 (1H, dd, $J=15.9$ Hz and $J=2.5$ Hz), 2.65 (1H, dd, $J=15.9$ Hz and $J=5.8$ Hz), 3.38 (2H, m), 3.74 (1H, m), 3.80 (3H, s), 4.04 (1H, d, $J=14.7$ Hz), 5.25 (1H, d, $J=14.7$ Hz), 6.88 (2H, d, $J=8.7$ Hz), 7.23 (2H, d, $J=8.7$ Hz). ^{13}C NMR ($CDCl_3$, 50 MHz) δ 19.84, 46.50, 47.13, 48.04, 48.81, 55.63, 114.55, 129.11, 129.81, 159.60, 166.36, 204.21.
14. Selected data for **5** ^{1}H NMR ($CDCl_3$, 200 MHz) δ 1.18 (3H, d, $J=6.6$ Hz), 2.98 (1H, dd, $J=16.1$ Hz and $J=1.9$ Hz), 3.47 (1H, dd, $J=16.1$ Hz and $J=5.9$ Hz), 3.81 (3H, s), 3.85 (m, 1H); 3.90 (3H, s), 4.02 (3H, s), 4.09 (1H, d, $J=14.6$Hz), 5.48 (1H, d, $J=14.6$Hz), 6.89 (2H, d, $J=8.5$ Hz), 7.16 (1H, s), 7.31 (2H, d, $J=8.5$ Hz), 7.38 (1H, s), 8.74 (1H, s). ^{13}C NMR ($CDCl_3$, 50 MHz) δ 18.80, 38.57, 48.08, 50.28, 55.61, 56.50, 56.57, 106.51, 107.53, 114.43, 121.32, 123.06, 129.73, 130.08, 135.45, 146.89, 150.11, 154.38, 154.38, 159.41, 163.56.
15. Selected data for **12** ^{1}H NMR ($CDCl_3$, 200 MHz) δ 1.13 (3H, d, $J=6.6$ Hz), 3.54 (1H, dd, $J=18.0$ Hz and 3.6 Hz), 3.65 (1H, dd, $J=18.0$ Hz and 6.3 Hz), 3.94 (1H, m), 4.00 (3H, s), 4.14 (3H, s), 4.16 (1H, d, $J=15.0$ Hz), 4.45 (3H, s), 5.36 (1H, d, $J=15.0$ Hz), 7.32 (5H, m), 7.42 (1H, s), 7.69 (1H, s), 9.30 (1H, s). ^{13}C NMR ($CDCl_3$, 50 MHz) δ 19.31, 34.13, 40.41, 48.53, 49.10, 56.69, 57.99, 99.07, 107.75, 121.92, 124.36, 127.85, 127.94, 128.89, 136.14, 139.48, 141.98, 151.95, 153.37, 159.27, 159.52.
16. Selected data for **2** ^{1}H NMR ($CDCl_3$, 200 MHz) δ 1.29 (3H, d, $J=6.5$ Hz), 2.13 (1H, d, $J=16.0$ Hz), 2.50 (1H, dd, $J=15.6$ Hz, $J=4.5$ Hz), 3.14 (3H, s), 3.43 (1H, m), 3.60 (1H, d, $J=18.5$ Hz), 3.84 (1H, d, $J=18.5$ Hz), 3.86 (3H, s), 3.87 (3H, s), 4.11 (d, 1H, $J=15$ Hz), 5.44 (d, 1H, $J=15$ Hz), 6.42 (1H, s), 6.68 (1H, s), 7.31 (5H, m).
17. Selected data for **15** ^{1}H NMR ($CDCl_3$, 200 MHz) δ 1.12 (3H, d, $J=6.6$ Hz), 2.90 (1H, dd, $J=15.6$ Hz and 1.7 Hz), 3.11 (3H, s), 3.37 (1H, dd, $J=15.6$ Hz, $J=5.8$ Hz), 3.79 (1H, m), 3.80 (3H, s), 4.03 (3H, s), 4.05 (3H, s), 4.07 (1H, d, $J=14.6$ Hz), 5.38 (1H, d, $J=14.6$ Hz), 6.88 (2H, d, $J=8.6$ Hz), 7.30–7.35 (4H, m). ^{13}C NMR ($CDCl_3$, 50 MHz) δ 18.38, 30.09, 39.78, 48.53, 49.92, 55.67, 56.45, 56.62, 103.28, 107.90, 114.47, 120.29, 123.94, 129.79, 130.50, 144.15, 145.62 149.86, 153.74, 155.01, 159.44, 164.59.
18. (a) Fehnel, E. A.; Deyrup, J. A.; Davidson, M. B. *J. Org. Chem.* **1958**, *23*, 1996; (b) Fehnel, E. A. *J. Org. Chem.* **1966**, *31*, 2899.
19. Selected data for *syn*-**13a** ^{1}H NMR ($CDCl_3$, 200 MHz) δ 1.12 (3H, d, $J=7.2$ Hz), 1.28 (3H, d, $J=6.6$ Hz), 2.58 (1H, dd, $J=16.6$ Hz and 3.7 Hz), 2.68 (1H, dd, $J=16.6$ Hz and 5.9 Hz), 3.25 (3H, s), 3.55 (1H, m), 3.86 (3H, s), 3.88 (3H, s), 3.89 (1H, d, $J=15.2$ Hz), 4.23 (1H, q, $J=6.5$ Hz), 5.44 (1H, d, $J=15.2$ Hz), 6.47 (1H, s), 6.74 (1H, s), 7.18–7.34 (5H, m). ^{13}C NMR ($CDCl_3$, 50 MHz) δ 18.24, 25.16, 30.49, 32.70, 33.41, 47.37, 48.69, 56.73 (2), 98.98, 104.56, 112.48, 122.04, 127.38, 128.13, 128.55, 134.09, 139.39, 143.37, 145.45, 147.79, 166.49.
20. For the rearrangement of the sulfinate intermediate, see: (a) Biellman, J. F.; Callot, H. J.; *Bull. Soc. Chem. Fr.* **1968**, 1154; (b) Caughey, W. S.; Schellenberg, K. A. *J. Org. Chem.* **1966**, *31*, 1978.
21. Vitry, C.; Bédat, J.; Prigent, Y.; Levacher, V.; Dupas, G.; Salliot, I.; Quéguiner, G.; Bourguignon, J. *Tetrahedron* **2001**, *57*, 9101–9108.